Centroid and envelope dynamics of high-intensity charged particle beams in an external focusing lattice and oscillating wobbler for heavy ion fusion applications

Hong Qin,[1,2] Ronald C. Davidson,[1] and B. Grant Logan[3]

[1]*Plasma Physics Laboratory, Princeton University, Princeton, NJ 08543, USA*

[2]*Department of Modern Physics, University of Science and Technology of China, Hefei, Anhui 230026, China*

[3]*Lawrence Berkeley National Laboratory, Berkeley, CA 94720*

Abstract

Recent heavy ion fusion target studies show that with an appropriate beam energy ramp and beam smoothing techniques, it may be possible to achieve ignition with direct drive and energy gain larger than 100 at 1MJ. To realize these advanced, high-gain heavy ion fusion schemes based on direct drive, it is necessary to develop a reliable beam smoothing technique to mitigate instabilities and facilitate uniform deposition on the target. The centroid dynamics of a high-intensity charged particle beam is investigated as a beam smoothing technique to achieve uniform illumination over a suitably chosen region of the target. The motion of the beam centroid projected onto the target follows a smooth pattern to achieve the desired illumination, for improved stability properties during the beam-target interaction. The centroid dynamics is controlled by an oscillating "wobbler", a set of electrically-biased plates driven by RF voltage. Using a model based on moments of the Vlasov-Maxwell equations, we show that the wobbler deflection force acts only on the centroid motion, and that the envelope dynamics are independent of the wobbler fields. If the conducting wall is far away from the beam, then the envelope dynamics and centroid dynamics are completely decoupled. This is an ideal situation for the beam wobbling technique, because the wobbler system can be designed to generate the desired centroid motion on the target without considering the potentially deleterious effects on the envelope and emittance. A conceptual design of the wobbler system for a heavy ion fusion driver is briefly summarized.

I. INTRODUCTION

Recent heavy ion fusion target studies show that with appropriate beam energy ramp and beam smoothing techniques, it may be possible to achieve ignition with direct drive and energy gain larger than 100 at 1MJ [1]. With the newly envisioned shock ignition method, it may be possible that an energy gain of 1000 could be achieved using 1.5MJ heavy ion direct drive [2]. To realize these advanced, high-gain heavy ion fusion schemes based on direct drive, it is important to develop a reliable beam smoothing technique to mitigate instabilities and facilitate uniform deposition. It has been proposed recently that the dynamics of the beam centroid can be explored as a possible beam smoothing technique [1, 3–6] to achieve a uniform illumination over a suitably chosen region of the target. The basic idea is to induce an oscillatory motion of the centroid for each transverse slice of the beam such that the centroids of different slices strike different locations on the target. The motion of the centroid projected onto the target is designed to follow a smooth pattern in order to achieve the desired uniform illumination over a suitably chosen region, *e.g.*, an annular region, for significantly improved stability properties during the target implosion phase [1, 7–9]. The improvement of stability properties can be attributed to two factors. First, uniform illumination reduces the initial seeding amplitude of the Rayleigh-Taylor instability. Secondly, at a given location on the target, the energy/momentum input is pulsating rapidly with time, which results in a dynamic stabilization effect for the instability.

The centroid dynamics is actively controlled by the deflection force imposed by a set of biased electrical plates, which are called "wobblers", because of the wobbling motion that they induce in the beam centroid motion. The bias voltage on the wobbler plates oscillates with time in order to deliver different beam slices to different locations on the target (See Fig. 1). In laser-driven inertial confinement fusion research, uniformity of laser illumination is also critically important, and sophisticated smoothing systems using distributed phase-plate technology have been developed [10]. The wobbler system for high-intensity beams described here is analogous to these smoothing systems for laser beams.

Beam dynamics is often studied in terms of envelope and centroid motions [11–15]. For example, unstable breathing modes can be described by envelope instabilities [11, 16], and the two-stream electron cloud instability [17, 18] and beam-beam interactions [19] are effectively modelled by following the centroid dynamics. Envelope dynamics is also employed

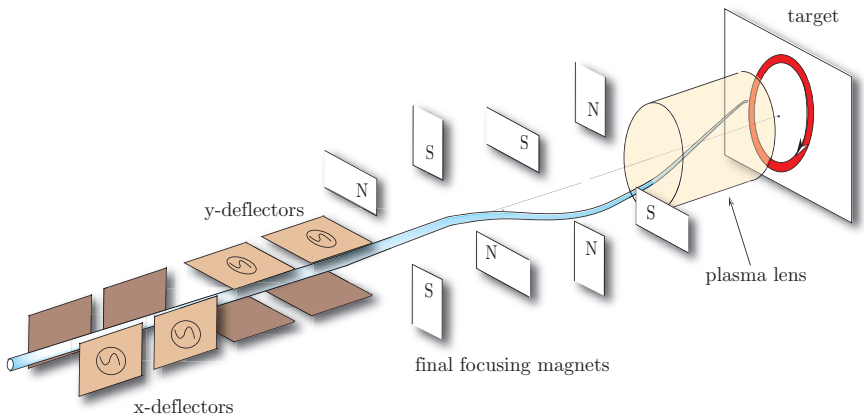

FIG. 1: Quadrupole focusing lattice and wobbler system with neutralizing plasma lens. The motion of the centroid projected onto the target follows a smooth pattern in order to achieve uniform illumination over a suitably chosen region of the target.

to design beam focusing systems [20, 21], while the purpose of studying centroid dynamics in most cases is to suppress instability or minimize the oscillations of the beam centroid around the design orbit [22]. From the point of view of the beam dynamics, the motions of the centroid and envelope represent different degrees of freedom. If the self-generated space-charge force is not strong, then the centroid dynamics and the envelope dynamics are decoupled. In this case, the centroid dynamics is described by the dynamical equations for a charged particle moving in the external focusing lattice and wobbler fields. For heavy ion fusion and high energy density physics applications, the beam intensity is high, and the effects of the self-generated space-charge force must be included. It is therefore necessary to determine the governing equations for the centroid dynamics for high-intensity beams, and ask whether the centroid dynamics is coupled to the beam envelope dynamics relative to the centroid motion. Another question is whether a realistic wobbler system using currently available technologies can be designed to achieve the desired wobbler motion on the target for a realistic heavy ion fusion driver. We will address these important questions regarding the centroid and envelope dynamics of high-intensity beams in an external focusing lattice and wobbler fields.

We start our study from the nonlinear Vlasov-Maxwell equations for high-intensity beams [23] in an external focusing lattice and a wobbler field. Two different approaches are adopted. The first approach is to derive a set of rate equations for the centroid, and the root-mean-square (rms) envelope and emittance, by taking appropriate moments of the Vlasov-Maxwell

equations. The second approach is to construct a generalized self-consistent Kapchinskij-Vladimirskij (KV) solution of the Vlasov-Maxwell equations including the envelope dynamics as well as the centroid dynamics. The external deflection force induced by the wobbler fields is included in the models, in addition to the transverse focusing lattice. Since the Vlasov-Maxwell equations are nonlinear, adding this additional physics could result in unexpected results. In order to systematically study the wobbler dynamics, we need to carry out a careful analysis of the Vlasov-Maxwell equations including simultaneously all of the relevant physics components, i.e., the wobbler fields, the focusing lattice, the space-charge force, and the emittance. Using these two models, we show that the wobbler deflection force acts only on the centroid motion, and that the envelope dynamics is independent of the wobbler fields. Furthermore, if the conducting wall is far away from the beam, then the envelope dynamics and the centroid dynamics are completely decoupled even when the space-charge force is strong. Based on these models, a conceptual design of the wobbler system for a heavy ion fusion driver is summarized. We demonstrate that a 10-meter-long, 67MHz RF field with 0.28MV/m field strength is able to impose enough transverse momentum to generate the desired wobbler motion on a 2.5mm target plane for a 2.43GeV Cs^+ beam with a 2895A peak current.

The paper is organized as follows. In Section II, the moment equations for the beam centroid and envelope are derived from the nonlinear Vlasov-Maxwell equations. The KV solution and associated centroid and envelope equations are presented in Section III. We outline a conceptual design example for the heavy ion fusion wobbler and final focusing system in Section IV.

II. MOMENT EQUATIONS FOR THE CENTROID AND ENVELOPE

In a quadrupole focusing lattice with wobbler fields, the transverse dynamics of a particle in laboratory-frame coordinates (x, y) is determined from [23]

$$x'' = -\kappa_x(s)\,x - \frac{\partial\psi}{\partial x} + F_x(s)\ , \tag{1}$$

$$y'' = -\kappa_y(s)\,y - \frac{\partial\psi}{\partial y} + F_y(s)\ , \tag{2}$$

where $\psi = e\phi/\gamma^3 m\beta^2 c^2$ is the normalized self-field potential, $\kappa_x(s) = \kappa_q(s)$ and $\kappa_y(s) = -\kappa_q(s)$ are the focusing strengths of the quadrupole lattice, and $F_x(s)$ and $F_y(s)$ are the transverse deflection forces due to the wobblers. The nonlinear Vlasov-Maxwell equations for the beam distribution function $f(s, x, y, v_x, v_y)$ and self-field potential ψ are [23]

$$\frac{\partial f}{\partial s} + v_x \frac{\partial f}{\partial x} + v_y \frac{\partial f}{\partial y} - \left(\kappa_x x + \frac{\partial \psi}{\partial x} - F_x\right) \frac{\partial f}{\partial v_x} - \left(\kappa_y y + \frac{\partial \psi}{\partial y} - F_y\right) \frac{\partial f}{\partial v_y} = 0, \tag{3}$$

$$\left(\frac{\partial^2}{\partial x^2} + \frac{\partial^2}{\partial y^2}\right) \psi = -\frac{2\pi K_b}{N_b} \int f \, dv_x dv_y \,, \tag{4}$$

where $N_b = \int f dv_x dv_y dx dy$ is the line density of the beam particles, and $K_b = 2N_b e^2/\gamma^3 m\beta^2 c^2$ is the self-field perveance. Here, m is the rest mass of a beam particle, γ is the relativistic mass factor, c is the speed of light in *vacuo*, and βc is the beam velocity. We assume that there is no longitudinal coupling between different slices of the beam, and that the nonlinear Vlasov-Maxwell equations (3) and (4) describe the transverse dynamics of each slice of the beam.

To derive the rms envelope equations and the centroid equations [11–15], we start from the rate equation for a phase-space moment of the Vlasov equation. Let $\chi(x, y, v_x, v_y, s)$ be any phase-space function, then the χ-moment of f is defined as

$$\langle \chi \rangle \equiv (\int \chi f \, dx dy dv_x dv_y)/N_b \,. \tag{5}$$

From Eq. (3), we obtain [23] the rate equation for $\langle \chi \rangle$

$$\frac{d\langle \chi \rangle}{ds} = \left\langle \frac{\partial \chi}{\partial s} + v_x \frac{\partial \chi}{\partial x} + v_y \frac{\partial \chi}{\partial y} - \left(\kappa_x x + \frac{\partial \psi}{\partial x} - F_x\right) \frac{\partial \chi}{\partial v_x} - \left(\kappa_y y + \frac{\partial \psi}{\partial y} - F_y\right) \frac{\partial \chi}{\partial v_y} \right\rangle . \tag{6}$$

The transverse displacement of the beam centroid is defined by the first moment of f with respect to displacement, *i.e.,*

$$\mu \equiv \langle x \rangle \,, \tag{7}$$

$$\nu \equiv \langle y \rangle \,. \tag{8}$$

Applying Eq. (6), we obtain

$$\mu' = \langle x \rangle' = \langle x' \rangle = \langle v_x \rangle \ , \tag{9}$$

$$\nu' = \langle y \rangle' = \langle y' \rangle = \langle v_y \rangle \ . \tag{10}$$

Letting $\chi = v_x$ and $\chi = v_y$ in Eq. (6), we acquire the dynamical equations for the centroid motion

$$\mu'' = \langle v_x \rangle' = -\kappa_x \mu + F_x - \left\langle \frac{\partial \psi}{\partial x} \right\rangle \ , \tag{11}$$

$$\nu'' = \langle v_y \rangle' = -\kappa_y \nu + F_y - \left\langle \frac{\partial \psi}{\partial y} \right\rangle \ . \tag{12}$$

It turns out that the rms envelope dimensions (a, b) and transverse emittances $(\varepsilon_x, \varepsilon_y)$ need to be defined relative to the centroid as

$$a \equiv \sqrt{\langle x - \mu \rangle^2} \, , \, \varepsilon_x \equiv 2\sqrt{a^2 \left\langle (v_x - \mu')^2 \right\rangle - \langle (v_x - \mu')(x - \mu) \rangle^2}, \tag{13}$$

$$b \equiv \sqrt{\langle y - \nu \rangle^2} \, , \, \varepsilon_y \equiv 2\sqrt{b^2 \left\langle (v_y - \nu')^2 \right\rangle - \langle (v_y - \nu')(y - \nu) \rangle^2} \, . \tag{14}$$

To derive the dynamics equations for a, we need the rate equations for $\chi = (x - \mu)^2 / 2$ and $\chi = (v_x - \mu')(x - \mu)$. For $\chi = (x - \mu)^2 / 2$, the rate equation is

$$\frac{1}{2} \frac{d}{ds} \left\langle (x - \mu)^2 \right\rangle = \frac{d}{ds} \frac{a^2}{2} = \left\langle - (x - \mu) \frac{\partial \mu}{\partial s} \right\rangle + \langle x' (x - \mu) \rangle = \langle (x' - \mu')(x - \mu) \rangle \ . \tag{15}$$

For $\chi = (v_x - \mu')(x - \mu)$, the corresponding rate equation is

$$\begin{aligned} \frac{d}{ds} \langle (v_x - \mu')(x - \mu) \rangle &= \left\langle (x' - \mu')^2 \right\rangle - \kappa_x (s) \left\langle (x - \mu)^2 \right\rangle \\ &\quad - \left\langle \frac{\partial \psi}{\partial x} (x - \langle x \rangle) \right\rangle + \langle F_x (x - \mu) \rangle \ . \end{aligned} \tag{16}$$

Taking another time-derivative on Eq. (15), we obtain

$$\begin{aligned} \frac{d^2}{ds^2} \frac{a^2}{2} &= \frac{d}{ds} \langle (x' - \mu')(x - \mu) \rangle \\ &= \left\langle (x' - \mu')^2 \right\rangle - \kappa_x (s) \left\langle (x - \mu)^2 \right\rangle - \left\langle \frac{\partial \psi}{\partial x} (x - \mu) \right\rangle + \langle F_x (x - \mu) \rangle \ . \end{aligned} \tag{17}$$

According the definition of ε_x in Eq. (13), the $\left\langle (x'-\mu')^2 \right\rangle$ term on the right-hand side of Eq. (17) can be expressed as

$$\left\langle (x'-\mu')^2 \right\rangle = \frac{\varepsilon_x^2}{4a^3} - \left(\frac{da}{ds}\right)^2 . \tag{18}$$

Then Eq. (17) can be re-written as the envelope equation for a,

$$a'' + \kappa_x a = \frac{\varepsilon_x^2}{4a^3} - \frac{1}{a}\left\langle \frac{\partial \psi}{\partial x}(x-\mu) \right\rangle . \tag{19}$$

To derive the dynamical equation for ε_x, we need the rate equation for $\chi = (v_x - \mu')^2$, *i.e.*,

$$\frac{d}{ds}\left\langle (v_x-\mu')^2 \right\rangle = \left\langle 2(x'-\mu')\left(-k_s(s)\,x - \frac{\partial \psi}{\partial x} + F_x\right)\right\rangle . \tag{20}$$

From the definition of ε_x, the time-derivative of ε_x^2 is

$$\begin{aligned} \frac{d}{ds}\frac{\varepsilon_x^2}{4} &= a^2 \frac{d}{ds}\left\langle (x'-\mu')^2 \right\rangle + \left\langle (x'-\mu')^2 \right\rangle \frac{da^2}{ds} \\ &\quad - 2\left\langle (x'-\mu')(x-\mu) \right\rangle \frac{d}{ds}\left\langle (x'-\mu')(x-\mu) \right\rangle . \end{aligned} \tag{21}$$

Making use of Eq. (20), Eq. (21) can be simplified to

$$\frac{d}{ds}\left(\frac{\varepsilon_x^2}{8}\right) = \left\langle \frac{\partial \psi}{\partial x}(x-\mu) \right\rangle \frac{d}{ds}\left(\frac{a^2}{2}\right) - a^2 \left\langle \frac{\partial \psi}{\partial x}(v_x-\mu') \right\rangle . \tag{22}$$

Eqs. (19) and (22) are the envelope equations for a and ε_x. Similarly, the dynamical equations for b and ε_y can be derived, and expressed as

$$b'' + \kappa_x b = \frac{\varepsilon_y^2}{4b^3} - \frac{1}{b}\left\langle \frac{\partial \psi}{\partial y}(y-\nu) \right\rangle , \tag{23}$$

$$\frac{d}{ds}\left(\frac{\varepsilon_y^2}{8}\right) = \left\langle \frac{\partial \psi}{\partial y}(y-\nu) \right\rangle \frac{d}{ds}\left(\frac{b^2}{2}\right) - b^2 \left\langle \frac{\partial \psi}{\partial y}(v_y-\nu') \right\rangle . \tag{24}$$

The evolution of the centroid dynamics, the rms envelope dimensions, and the transverse emittances are determined from Eqs. (11), (12), (19), and (22)-(24). From Eqs. (19) and (23), it is clear that the deflection force imposed by the wobbler fields does not directly affect the envelope dynamics and emittances. Furthermore, if the conducting wall is far

away from the beam, or if image-charge effects are negligible, then it can be shown that the self-field terms in Eqs. (11) and (12) vanish [see Eq. (28)], and the self-field potential ψ in Eqs. (22) and (24) is a function of $(x-\mu, y-\nu)$ only, which indicates that the self-field force does not affect the centroid dynamics, and the evolution of the envelope dimensions and emittances is independent of the centroid motion. In this case, there is a complete decoupling between the centroid dynamics and the dynamics of the envelope dimensions and emittances. The centroid motion is affected only by the focusing lattice and wobbler fields, and the envelope dimensions and emittances evolve as if there were no wobbler fields and no centroid dynamics. This is an ideal situation for the envisioned applications of the beam wobbling technique, because the wobbler system can be designed to generate the desired centroid motion on the target without considering the potentially deleterious effects on the envelope and emittance.

However, if the conducting wall is not far removed from the beam, then the dynamics of the centroid, the envelope dimensions and emittances are coupled through the self-field force. To determine the self-field force on the beam centroid, we note that in Eqs. (11) and (12),

$$-\left(\left\langle\frac{\partial\psi}{\partial x}\right\rangle, \left\langle\frac{\partial\psi}{\partial y}\right\rangle\right) = -\left\langle\nabla\psi\right\rangle = \int -f\nabla\psi dv_x dv_y dxdy = -\int_V n\nabla\psi dxdy. \tag{25}$$

Using the fact that

$$-n\nabla\psi = \frac{N_b}{2\pi K_b}(\nabla\cdot\nabla\psi)\nabla\psi = \frac{N_b}{2\pi K_b}\left[\nabla\cdot(\nabla\psi\nabla\psi) - (\nabla\psi\cdot\nabla)\nabla\psi\right] \tag{26}$$

and

$$\nabla\frac{|\nabla\psi|^2}{2} = (\nabla\psi\cdot\nabla)\nabla\psi\,, \tag{27}$$

we can express the self-field force as a surface integral over the conducting wall,

$$-\left\langle\nabla\psi\right\rangle = \frac{N_b}{2\pi K_b}\int_{wall}\left(\nabla\psi\nabla\psi - |\nabla\psi|^2\,\mathbf{I}\right)\cdot d\mathbf{s}\,. \tag{28}$$

Here $\mathbf{I}$ is the unit tensor. Equation (28) states that the self-field force on the centroid motion is determined by the self-field on the conducting wall. As the conducting wall approaches infinity, the self-field force vanishes. For the self-field force terms in Eqs. (19) and (22)-(24),

ψ will depend on $(x-\mu, y-\nu)$ as well as (μ,ν) if the conducting wall is nearby, and the centroid dynamics will affect the dynamics of the envelope dimensions and emittances. This effect should be minimized in the design of wobbler systems. The image charge effect has been previously analyzed in Ref. [13], and the equations employed in CIRCE [14] show that the equations become decoupled when the pipe radius is set to infinity.

Assuming that the conducting wall is far away from the beam, then in the coordinate system centered at the centroid, $X = x-\mu$, $Y = y-\nu$, we find that the envelope equations and the emittance equations are exactly the same as those in the laboratory coordinate system in the absence of centroid dynamics [6]. Therefore, known results for the latter case can be applied directly to Eqs. (19) and (22)-(24). A particularly important result is for the case where the beams have fixed-shape density profiles. Assume that the density profile of the beam has the following fixed-shape form

$$n\left(X,Y,s\right) = \frac{N_b}{2\pi ab} S\left(\frac{X^2}{2a^2}+\frac{Y^2}{2b^2}\right) , \tag{29}$$

where S is the density shape function. It can then be shown [23] that Eqs. (19) and (23) reduce exactly to

$$a'' + \kappa_x a = \frac{\varepsilon_x^2}{4a^3} - \frac{K_b}{2(a+b)} , \tag{30}$$

$$b'' + \kappa_x a = \frac{\varepsilon_y^2}{4b^3} - \frac{K_b}{2(a+b)} . \tag{31}$$

III. KV DISTRIBUTION AND ASSOCIATED CENTROID AND ENVELOPE EQUATIONS

In the last section, we showed that when the conducting wall is far away, the envelope equations relative to the centroid is similar to the those without the centroid freedom. Since for the later case there is a corresponding self-consistent KV solution of the nonlinear Vlasov-Maxwell equations, this similarity suggests that a self-consistent KV solution to the nonlinear Vlasov-Maxwell equations may exist for high-intensity beams including the centroid dynamics in an external focusing lattice and wobbler fields. We now show that this is indeed true [6].

Because the self-field potential ψ and the distribution function is nonlinearly coupled in

the Vlasov-Maxwell equations, to construct the self-consistent solution, we first assume a specific form for the self-field potential ψ, and find the invariants of the particle dynamics in the external field and the self-field. Any function of the invariants as a distribution function in the phase space is a solution of the Vlasov equation. However, an arbitrary distribution function constructed this way will not generate the self-field potential ψ assumed. We will select a specific distribution function of the invariants and verify that it indeed generates the initially assumed self-field potential ψ. Then a self-consistent solution is found, and the Vlasov-Maxwell equations in the phase space are reduced to a set of envelope equations that are ordinary differential equations in terms of time. For a high-intensity beam in a quadrupole lattice and wobbler fields, we first assume the self-field force to be linear in the centroid frame, *i.e.*,

$$\frac{\partial\psi}{\partial x} = \frac{-2K_b\,(x-\mu)}{\bar{a}(\bar{a}+\bar{b})},\ \frac{\partial\psi}{\partial y} = \frac{-2K_b\,(y-\nu)}{\bar{b}(\bar{a}+\bar{b})}, \tag{32}$$

which is equivalent to assume the self-field potential to be

$$\psi = -\frac{K_b}{(\bar{a}+\bar{b})}\left[\frac{(x-\mu)^2}{\bar{a}^2} + \frac{(y-\nu)^2}{\bar{b}^2}\right]. \tag{33}$$

Here, (μ,ν) is the centroid and $(\bar{a},\bar{b})$ is the envelope dimension in the centroid frame that need to be determined. It will be clear later that $\bar{a}$ and $\bar{b}$ are related to the rms envelope dimensions a and b through $\bar{a} = \sqrt{2}a$ and $\bar{b} = \sqrt{2}b$. For the centroid, we let the centroid motion satisfy

$$\mu'' + \kappa_x\mu - F_x = 0\,, \tag{34}$$

$$\nu'' + \kappa_y\nu - F_y = 0\,, \tag{35}$$

then from Eqs. (1), (2), (34) and (35), it follows that X and Y, the displacement relative to the centroid, evolve according to

$$X'' + \left[\kappa_x - \frac{2K_b}{\bar{a}(\bar{a}+\bar{b})}\right]X = 0\,, \tag{36}$$

$$Y'' + \left[\kappa_y - \frac{2K_b}{\bar{b}(\bar{a}+\bar{b})}\right]Y = 0\,. \tag{37}$$

Since Eqs. (36) and (37) are linear in X and Y, they admit the Courant-Snyder invariants

for the X and Y motions, *i.e.*,

$$A_X = \frac{\varepsilon_x^2 X^2}{\bar{a}^2} + \varepsilon_x^2 \left(\bar{a}X' - X\bar{a}'\right)^2 = const.,$$
$$A_Y = \frac{\varepsilon_y^2 Y^2}{\bar{b}^2} + \varepsilon_y^2 \left(\bar{b}Y' - Y\bar{b}'\right)^2 = const., \tag{38}$$

where ε_x and ε_y are constants corresponding to the conserved transverse emittances, and $\bar{a}$ and $\bar{b}$ are determined from the envelope equations

$$\bar{a}'' + \kappa_x \bar{a} - \frac{2K_b}{(\bar{a}+\bar{b})} = \frac{\varepsilon_x^2}{\bar{a}^3}\,, \tag{39}$$

$$\bar{b}'' + \kappa_y \bar{b} - \frac{2K_b}{(\bar{a}+\bar{b})} = \frac{\varepsilon_y^2}{\bar{b}^3}\,. \tag{40}$$

Any function of A_x and A_y is an exact solution of the Vlasov equation (3). But we also need the distribution function to generate the linear self-field force assumed in Eq. (32). We now show that the choice of distribution function [23]

$$f = \frac{N_b}{\pi^2 \varepsilon_x \varepsilon_y} \delta\left(\frac{A_X}{\varepsilon_x} + \frac{A_Y}{\varepsilon_y} - 1\right) \tag{41}$$

has this property. To verify this fact, we first calculate the density

$$n\left(X, Y, s\right) = \int f dv_x dv_y = \begin{cases} N_b/\pi\bar{a}\bar{b},\ X^2/a^2 + Y^2/b^2 \leq 1\,, \\ 0,\ X^2/a^2 + Y^2/b^2 > 1\,. \end{cases} \tag{42}$$

The density profile is spatially uniform inside of the elliptical cross-section beam, which indeed generates the initially assumed self-field potential in Eq. (33), upon solving Poisson's equation (4). Note that the KV distribution does not follow directly from the moment equations for the envelope and centroid because the moment equations do not specify the distribution function, and finding a distribution function that solves the Vlasov-Maxwell equations is generally non-trivial. Working together, with the moment equations and the KV solution give a leading-order description of the wobbler dynamics.

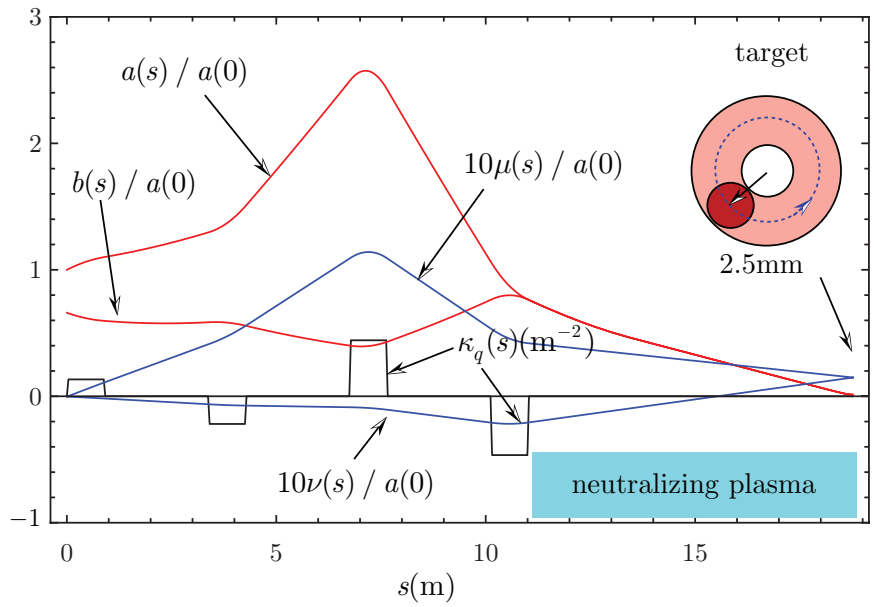

FIG. 2: Final focus and wobbler system for an illustrative heavy ion fusion driver [6]. The vertical scale for κ_q is m^{-2}. The envelope dimensions (a, b) are normalized by the initial beam envelope dimension $a(0)$. The centorid positions (μ, ν) are normalized by $a(0)/10$ for better illustration.

IV. CONCEPTUAL DESIGN EXAMPLE OF A HEAVY ION FUSION WOBBLER AND FINAL FOCUSING SYSTEM

As an example, we give a conceptual design of a final focus and wobbler system for a heavy ion fusion driver. The layout of the system is illustrated in Fig. 2. For simplicity, we assume that at $s = 0$, the wobbler fields (not shown) imposes a transverse momentum to the beam centroid. The beam then propagates through the final focus magnets with focusing strength $\kappa_q(s)$, and is focused onto the target at $s = 19\,\mathrm{m}$, with transverse spot size $a = b = 1.2\mathrm{mm}$. The initial envelope dimensions at $s = 0$ are $(a, b) = (4\,\mathrm{cm}, 2.28\,\mathrm{cm})$. The region between $s = 11\,\mathrm{m}$ and $s = 19\,\mathrm{m}$ is filled with pre-formed plasma which neutralizes the space-charge potential of the beam, but not the current [20]. As a result, the size of the beam continues to decrease before it strikes on the target. This is the familiar effect of a plasma lens. The beam is a Cs^+ beam with rest mass $m = 132.9\mathrm{au}$, kinetic energy $(\gamma - 1)\,mc^2 = 2.43\mathrm{GeV}$, and current $I = 2895\mathrm{A}$. The normalized strength $\hat{\kappa}_q$ of the four quadrupole magnets is $0.13\,\mathrm{m}^{-2}, 0.22\,\mathrm{m}^{-2}, 0.44\,\mathrm{m}^{-2}$,and $-0.47\,\mathrm{m}^{-2}$. These parameters are for the heavy ion fusion driver design described in Ref. [21]. The wobbler fields induce different transverse momenta for different slices according to oscillatory sinusoidal forces at $s = 0$. The forces in the x-

and y-directions has a $\pi/2$ phase difference. Therefore, the beam centroid traces out a circle on the target. The centroid dynamics illustrated in Fig. 2 corresponds to the slice where $(\mu, \nu) = (1.77\,\mathrm{mm}, 1.77\,\mathrm{mm})$ on the target, and the normalized momentum input by the wobbler fields is $(\mu', \nu') = (6.27 \times 10^{-4}, -0.85 \times 10^{-4})$ at $s = 0$. The radius of the centroid circle is 2.5mm. For a beam pulse of 15 ns long, the frequency of the wobbler fields is 67MHz. Assuming the effective length of the wobbler field is 10m, the RF field strength required is 0.30MV/m. These parameters are achievable with current technology. If the wobbler fields are placed in the upstream of the beam before the longitudinal compression [21], then a lower frequency can be used.

V. CONCLUSIONS

In summary, a fully self-consistent solution for high-intensity charged particle beams in a quadrupole lattice with wobbler fields is given by Eqs. (41), (39), and (40), and the centroid dynamics is determined from Eqs. (34) and (35). The deflection force imposed by the wobbler fields acts only on the centroid, and the self-consistent space-charge field only affects the envelope motion. This is consistent with the analysis leading to the rms envelope equations including the centroid dynamics. These conclusions and the corresponding envelope equations and centroid equations are expected to serve as theoretical tools in designing beam wobbler systems for applications to higher energy density physics and heavy ion fusion. The KV solution to the nonlinear Vlasov-Maxwell equations considered in this paper corresponds (exactly) to the case where the beam has a flat-top density profile. For more general choices of distribution function corresponding to beams with density profiles that are not flat-top, we expect that the rms envelope equations and the associated centroid equations derived by taking appropriate moments of the Vlasov-Maxwell equations remain a good approximation, particularly if the change in beam emittance remains small [24]. In practice, several non-ideal effects may exist. When the envelope amplitude is large, the effects associated with lens nonlinearities and kinetic effects can couple the centroid and envelope dynamics. The error field of the wobbler should be considered as well. To leading order, the error field correction can be modeled as a linear focusing force which modifies the definition of the focusing strengths κ_x and κ_y in Eqs. (1) and (2).

Acknowledgments

This research was supported by the U.S. Department of Energy.

---

[1] B. G. Logan, L. J. Perkins, and J. J. Barnard, Physics of Plasmas **15**, 072701 (2008).

[2] B. G. Logan, *et al.*, to be published.

[3] B. Sharkov, Nucl. Instr. Methods Phys. Res. **A577**, 14 (2007).

[4] D. H. H. Hoffmann (2009), private communication.

[5] H. Qin and R. C. Davidson, in *Proceedings of the 2009 Particle Accelerator Conference* (IEEE, New York, 2009).

[6] H. Qin, R. C. Davidson, and B. G. Logan, Phy. Rev. Lett. **104**, 254801 (2010).

[7] S. Kawata, T. Sato, T. Teramoto, E. Bandoh, Y. Masubichi, and I. Takahashi, Laser and Particle Beams **11**, 757 (1993).

[8] A. R. Piriz, N. A. Tahir, D. H. H. Hoffmann, and M. Temporal, Physical Review E **67**, 017501 (2003).

[9] A. R. Piriz, M. Temporal, J. J. L. Cela, N. A. Tahir, and D. H. H. Hoffmann, Plasma Phys. Control. Fusion **45**, 17331745 (2003).

[10] S. Skupsky, T. Kessler, S. Letzring, and Y. Chuang, Journal of Applied Physics **73**, 2678 (1993).

[11] S. Lund and B. Bukh, Physical Review Special Topics - Accelerators and Beams **7**, 1 (2004).

[12] S. Lund and J. J. Barnard (2009), U.S. Part. Accel. Shool Lecture Notes.

[13] E. Lee, E. Close, and L. Smith, in *Proceedings of the 1987 Particle Accelerator Conference* (IEEE, New York, 1988), p. 1186.

[14] W. Sharp, J. Barnard, and S. Yu, Particle Accelerators **37-38**, 205 (1992).

[15] J. Barnard, in *Proceedings of the 1995 Particle Accelerator Conference* (IEE, New York, 1996), p. 3241.

[16] S. Bernal, H. Li, R. Kishek, B. Quinn, M. Walter, M. Reiser, P. OShea, and C. Allen, Physical Review Special Topics - Accelerators and Beams **9**, 1 (2006).

[17] D. Neuffer, E. Colton, D. Fitzgerald, T. Hardek, R. H. andR. Macek, M. Plum, H. Thiessen, and T. S. Wang, Nucl. Instr. Methods Phys. Res. **A321**, 1 (1992).

[18] R. Zimmermann, Physical Review Special Topic - Accelerators and Beams **7**, 124801 (2004).

[19] J. Qiang, M. Furman, and R. Ryne, Journal of Computational Physics **198**, 278 (2004).

[20] A. Friedman, J. Barnard, R. Briggs, R. Davidson, M. Dorf, D. Grote, E. Henestroza, E. Lee, M. Leitner, and B. Logan, Nucl. Instr. Methods Phys. Res. **A606**, 6 (2009).

[21] H. Qin, R. C. Davidson, J. J. Barnard, and E. P. Lee, Physical Review Special Topics - Accelerators and Beams **7**, 104201 (2004).

[22] B. Blind and J. D. Gilpatrick, in *Proceedings of 2007 Particle Accelerator Conference* (IEEE, New York, 2007), pp. 4093–4095.

[23] R. C. Davidson and H. Qin, *Physics of Intense Charged Particle Beams in High Energy Accelerators* (Imperial College Press and World Scientific, 2001).

[24] M. A. Dorf, R. C. Davidson, E. A. Startsev, and H. Qin, Phys. Plasmas **16**, 123107 (2009).